Supporting Information

Sackmann et al. 10.1073/pnas.1324043111

SI Materials and Methods

Human Blood Draw and Neutrophil Isolation for Capture Experiments. Neutrophils were prepared from heparinized peripheral blood obtained from adult donors. Neutrophils were isolated by density fractionation over Percoll 1.090 μg/mL. The cell pellets were collected, and contaminating red blood cells were lysed by hypotonic lysing. Purified neutrophils were on average >95% pure and the contaminating cells were eosinophils.

Fraction of Exhaled Nitric Oxide Measurements. Fractions of exhaled nitric oxide (FeNo) measurements were collected just before blood draw. FeNO values were measured during a 10- to 15-s exhalation using the NIOX-MINO (Aerocrine Inc.) analyzer, according to the manufacturer's instruction. Briefly, patients were instructed to be seated with no nose clip, and to fully exhale away from mouthpiece. Patients then inhaled on the mouthpiece, maintaining a tight lip seal, to near total lung capacity over ∼2–3 s. Once total lung capacity was achieved, patients were instructed to slowly exhale keeping a constant flow for 10–15 s while continuing to maintain a tight lip seal. FeNO value was obtained by only one measurement, according to the manufacturer's instruction.

Spirometry Measurements. Spirometry was performed and analyzed according to currently approved American Thoracic Society Guidelines (1). Briefly, forced expiratory volume for 1 s (FEV1) and forced vital capacity (FVC) were collected using a nSpire KOKO spirometer (nSpire Health, Inc.), and the best FVC and FEV1 values from three reproducible measurements were used. FEV1 % predicted was determined using NHANES III-derived data. Reversibility was determined by change in FEV1 or FVC after four puffs of albuterol were administered and the subject rested for 10 min.

Device Fabrication in Polydimethylsiloxane and Polystyrene. Microfluidic devices were fabricated out of both polydimethylsiloxane (PDMS) and polystyrene. The master for the microfluidic base and lid of the diagnostic chip were fabricated using soft lithography methods with PDMS (Sylgard 164; Dow Corning). First, multilayer molds were created using SU-8 negative photoresist (MicroChem). Briefly, pattern designs were created using Adobe Illustrator (Adobe) and printed on film (Imagesetter). A first layer was spun according to the manufacturer's specifications on a 150-mm-diameter silicon wafer (WRS) using SU-8 50 to achieve 80-μm thickness. The photoresist was baked on hot plate and an OmniCure S1000 UV light source (EXFO) was used to transfer the pattern to the photoresist. After a post-exposure baking step, the second, 400-μm-thick layer was spun on the wafer and patterned. The mold was then developed for 4 h in SU-8 developer (PGMEA, 537543; Sigma) and washed with acetone and isopropyl alcohol. PDMS was prepared in a ratio of 10:1 base to cross-linking agent, degassed in vacuum, and poured over the SU-8 silicon mold on a hot plate. A transparency (Cheap Joe's), a layer of silicone (McMaster Carr), and a 5-kg weight were placed on top of the mold and baked at 80 °C for 4 h. The base and lid of the diagnostic device were adhered to non–tissue culture-treated plastic from a Petri dish (NUNC) before use. Photolithography masks used by the authors to fabricate devices are available upon request. For polystyrene devices, hot embossing fabrication techniques were used as previously described (2). A mold for the lid of the diagnostic device was rapid prototyped (FineLine Prototyping) from a source file created by SolidWorks (Dassault Systèmes SolidWorks Corp.) and then converted into an epoxy mold for hot embossing (2).

Preparation of Hydrogel–Chemoattractant Mixture. N-formyl-methionine-leucine-phenylalanine (fMLP; F3506-10MG, Sigma-Aldrich) was suspended in DMSO (D2650; Sigma-Aldrich) at 10 mM and stored at −80 °C. The hydrogel–chemoattractant (H-CA) mixture consisted of fMLP and Matrigel, mixed in a 1:1 ratio to a final gel concentration of 4 mg/mL. The H-CA mixture was prepared before each chemotaxis experiment. For all doses of chemoattractant, the fMLP dilution was performed in PBS (Invitrogen) before mixing with the hydrogel.

Calculating Chemotaxis Outputs. See Movie S2 for visual demonstration of generating the chemotaxis outputs. The absolute speed, chemotactic index, and chemotaxis velocity (or directional velocity toward the formation of the gradient of chemoattractant) of a tracked neutrophil were calculated using Eqs. **S1**–**S3**, where n is the number of frames of the time-lapse image, t_i is the time interval between frames i-1 and i; ∂x_i and ∂y_i are the displacements along the x and y axis, respectively, between times i-1 and i; and ΔT is the time interval between the first and last frame of the time lapse.

$$\text{speed} = \sum_{i=1}^{n} \frac{\sqrt{\delta x_i^2 + \delta y_i^2}}{n \delta t_i} \qquad \textbf{[S1]}$$

$$\text{CI} = \frac{\sqrt{(x_n - x_0)^2 + (y_n - y_0)^2}}{\sum_{i=1}^{n} \sqrt{\delta x_i^2 + \delta y_i^2}} \qquad \textbf{[S2]}$$

$$\text{directional velocity} = \frac{1}{n \Delta T} \sum_{i=1}^{n} \delta x_i \qquad \textbf{[S3]}$$

Microscopy. For all time-lapse experiments, phase contrast images were taken using an Olympus IX-81 optical microscope with a 10× objective and a numerical aperture of 0.30; the images were captured using a SPOT RT Monochrome CCD camera (Diagnostic Instruments, Inc.). The time-lapse experiments were conducted in an incubation chamber at 37 °C; before the start of an imaging session, the samples were allowed to warm to 37 °C for a minimum of 15 min. SlideBook software (Intelligent Imaging Innovations) was used to capture the time-lapse images. The data were exported in tif format and processed using Je'Xperiment (JEX) software. The imaging medium was dry for all images shown in this work.

Capture Efficiency Experiments. Neutrophils (at ∼1×10^6 cells per milliliter density) were purified (details in *Human Blood Draw and Neutrophil Isolation for Capture Experiments*) and then tagged with calcein-AM stain (L-3224; Invitrogen). The calcein-AM was prepared by mixing 1 μL of calcein-AM with 1 mL of PBS. Cells were then placed into the diluted calcein-AM and incubated at 37 °C for 8 min. Three microliters of the tagged cells were then resuspended into 15 μL of whole blood and injected into the microchannels. Phase contrast and fluorescent images were taken of six microchannels before washing, and then the normal washing procedure was performed. Images of the microchannels were taken again after washing. Cells were counted

manually using the ImageJ plug-in Cell Counter for both the pre- and postwashed channels. Count data from six channels were averaged, yielding an average count for a single experimental output ($n = 1$). Three replicates ($n = 3$) were performed. The capture efficiency was calculated by dividing the average number of neutrophils captured after washing was performed by the average number of neutrophils before washing was performed.

Neutrophil Enrichment on the Microfluidic Device. Following the neutrophil tagging steps outlined in the previous section, whole blood was injected with tagged neutrophils into eight P-selectin–coated microchannels. Additional blood was passed through microchannels, separated by 30 s, with sets of two microchannels receiving an additional whole-blood sample. Therefore, the first set of microchannels received 1 μL of whole blood each, the second set of two microchannels received 2 μL of whole blood each, the third set of two microchannels received 3 μL of whole blood each, and the fourth set of two microchannels received 4 μL of whole blood each. After allowing neutrophils to capture for 4 min, erythrocytes were removed by performing three washes with 3 μL of PBS, alternating the aspiration of PBS–blood mixture between the input and output ports. Cells were counted manually using the ImageJ plug-in Cell Counter.

Statistical Analysis. The associations between asthma diagnosis and chemotaxis outputs (speed, chemotactic index, and chemotaxis velocity) were examined using the Wilcoxon rank-sum test. The sensitivity and specificity for asthma diagnosis at varying thresholds of chemotactic velocity were summarized using the receiver operator characteristic curve. The optimal chemotaxis velocity threshold for asthma diagnosis was chosen to maximize the sum of specificity and sensitivity. Confidence intervals for sensitivity and specificity were constructed using 2,000 stratified bootstrap replicates (3). Each chemotaxis output was individually measured for 3–6 microchannels per subject, and the channel output values were averaged to yield a single value for each subject. Analyses were conducted using Mstat version 5.5 (www.mcardle.wisc.edu/mstat/) and R version 2.14 (www.R-project.org/). A two-sided P value less than 0.05 was regarded as significant.

1. Miller MR, et al.; ATS/ERS Task Force (2005) Standardisation of spirometry. *Eur Respir J* 26(2):319–338.
2. Young EWK, et al. (2011) Rapid prototyping of arrayed microfluidic systems in polystyrene for cell-based assays. *Anal Chem* 83(4):1408–1417.
3. Robin X, et al. (2011) pROC: An open-source package for R and S+ to analyze and compare ROC curves. *BMC Bioinformatics* 12:77.

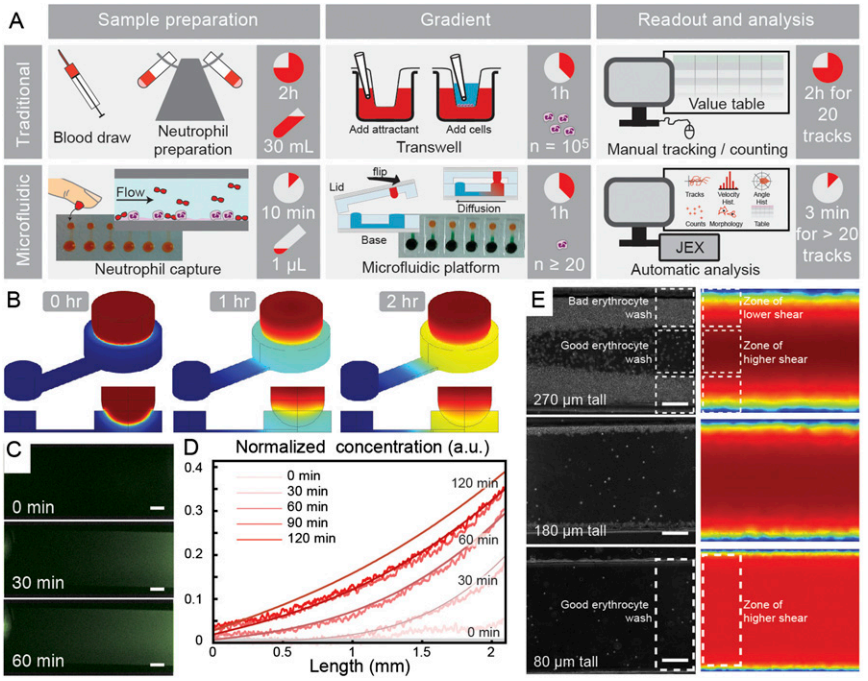

Fig. S1. Principles of the operation and function of the asthma characterization device. (*A*) Comparison of the purification and chemotaxis protocols for the asthma characterization device and Transwell assay. (*B*) Modeling (COMSOL multiphysics software) showing the formation of a chemical gradient. (*C*) Experimental results showing gradient formation of Alexa Fluor 488 dye. (*D*) Experiment and modeling found to be in close agreement for the formation of the chemical gradient. (*E*) Experiment and modeling showing the purification of neutrophils from erythrocytes is heavily dependent on the aspect ratio of the microfluidic device. Modified from ref. 1.

1. Sackmann EK et al. (2012) Microfluidic kit-on-a-lid: A versatile platform for neutrophil chemotaxis assays. *Blood* 120(14):e45–e53.

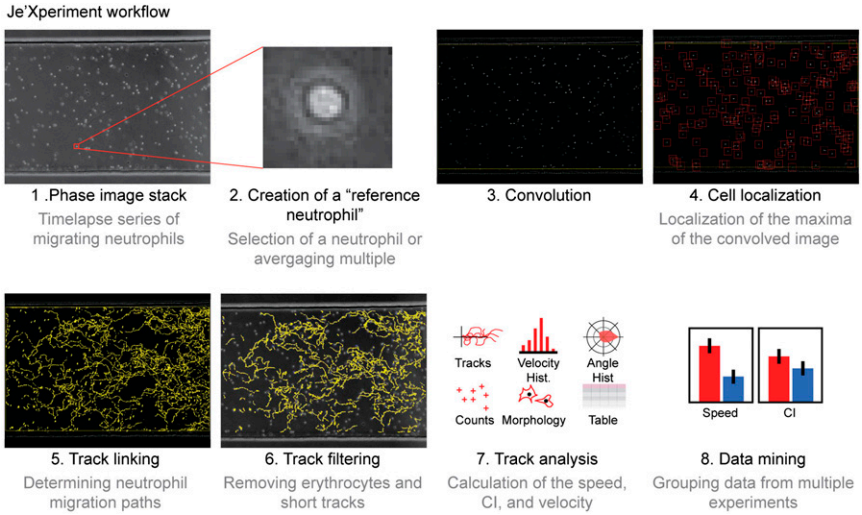

Fig. S2. JEX analysis workflow. JEX begins with the initial image in the time lapse (1); then the user selects a target cell (2); then the software performs a convolution (3) and locates the cells based on the convolved image (4). The cells are tracked from frame to frame (5), and filtering can be applied to further remove erythrocytes or cells that were not well-tracked (6). The software outputs a list of position vectors for each track and automatically yields outputs of interest (7) and has an interface to compare data over multiple samples and outputs (8). Modified from ref. 1.

1. Sackmann EK et al. (2012) Microfluidic kit-on-a-lid: A versatile platform for neutrophil chemotaxis assays. *Blood* 120(14):e45–e53.

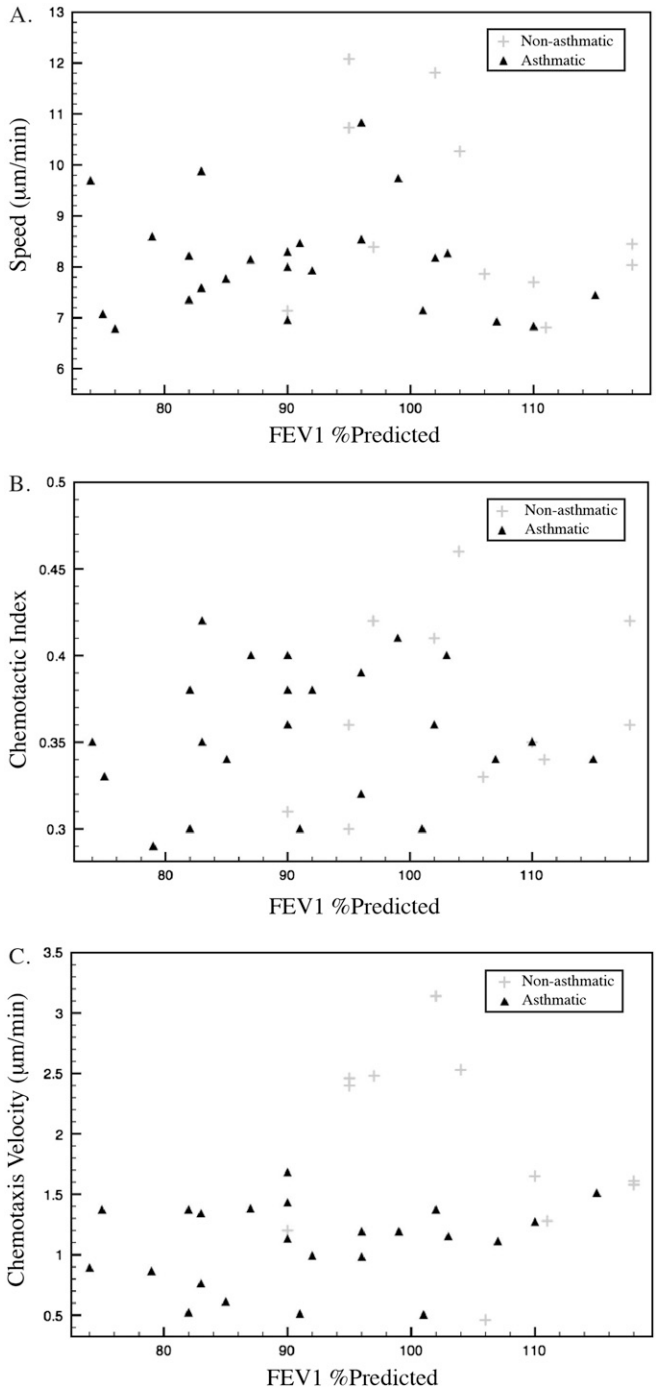

Fig. S3. FEV1 % predicted compared with neutrophil chemotaxis speed (*A*), chemotactic index (*B*), and (*C*) chemotaxis velocity. The speed and chemotactic index do not show any correlations with FEV1 % predicted for asthmatic and nonasthmatic patients. Patients with higher neutrophil chemotaxis appear to correlate with higher values of FEV1 % predicted.

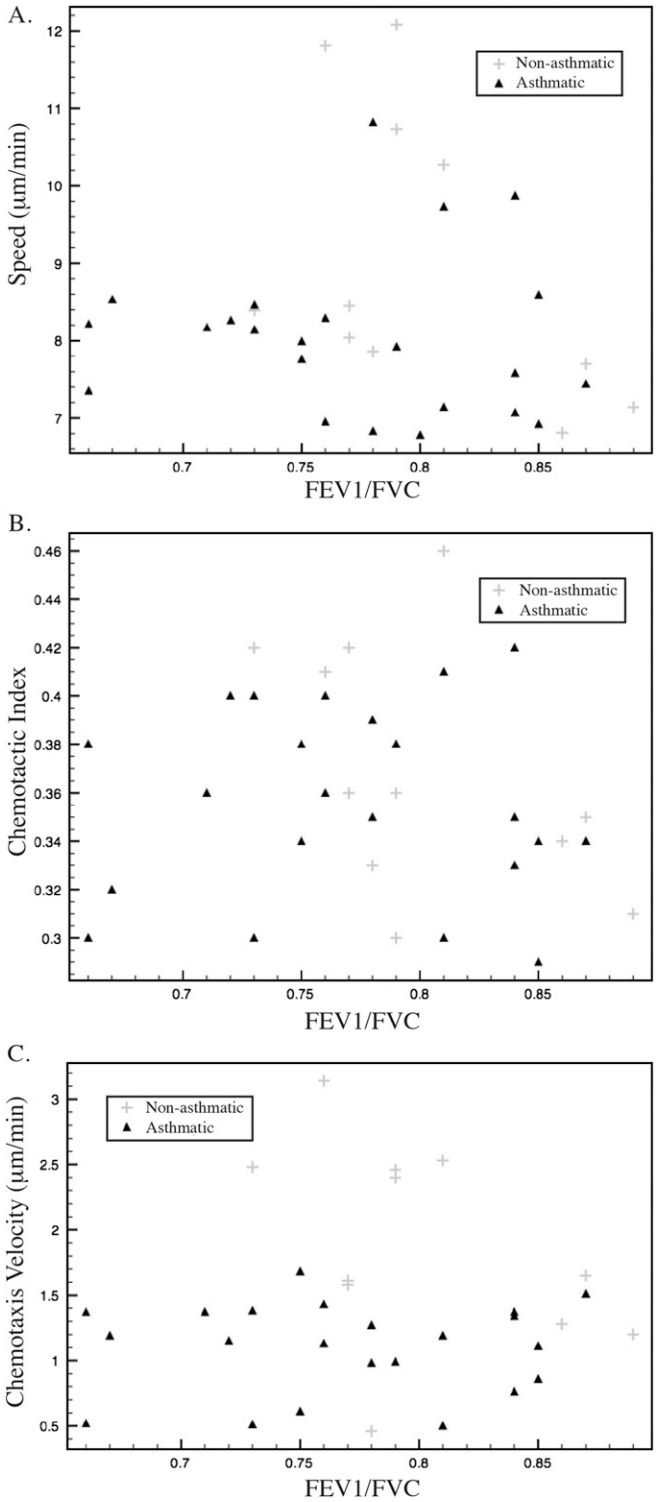

Fig. S4. FEV1/FVC compared with neutrophil chemotaxis speed (*A*), chemotactic index (*B*), and (*C*) chemotaxis velocity. No apparent correlations between the neutrophil chemotaxis outputs (*A*–*C*) and FEV1/FVC measurements. Asthmatic and nonasthmatic patients have spirometry measurements that span across the full range of FEV1/FVC values, and there are no apparent correlations between neutrophil chemotaxis and FEV1/FVC values.

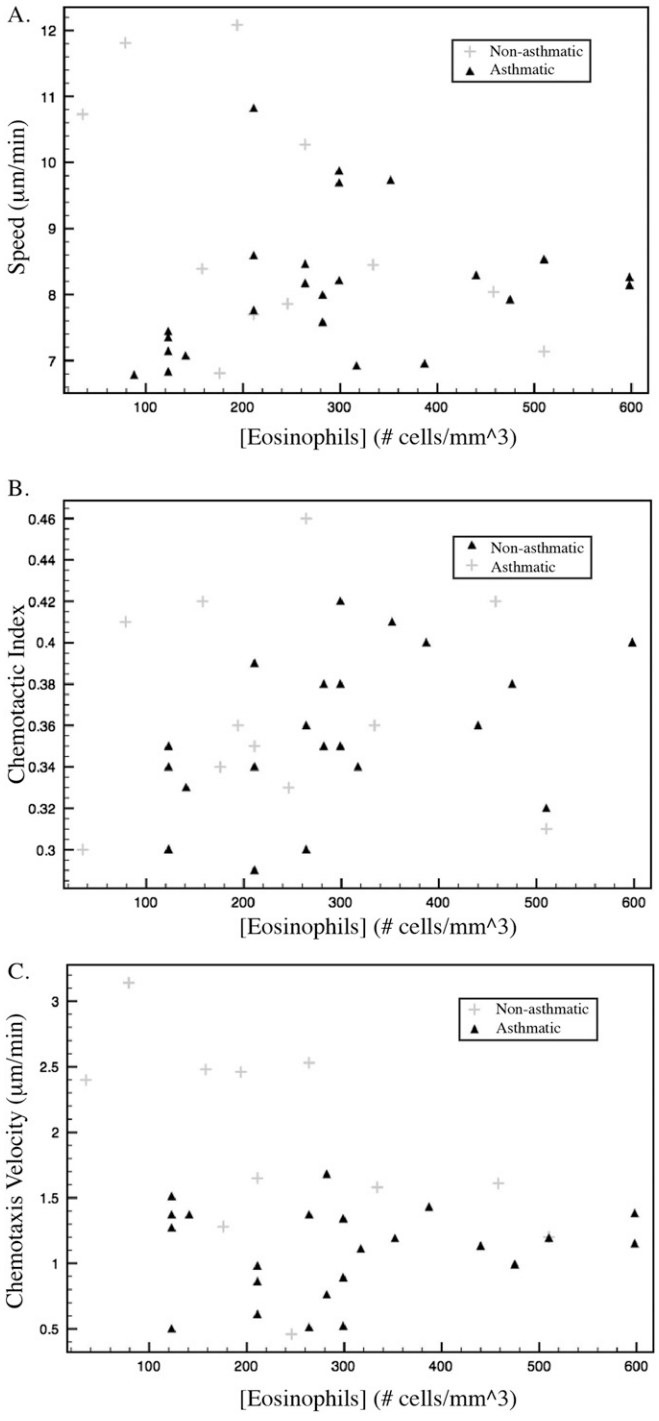

Fig. S5. Concentration of eosinophils in peripheral blood compared with neutrophil chemotaxis speed (*A*), chemotactic index (*B*), and (*C*) chemotaxis velocity. No apparent correlations between the neutrophil chemotaxis outputs (*A*–*C*) and eosinophil counts.

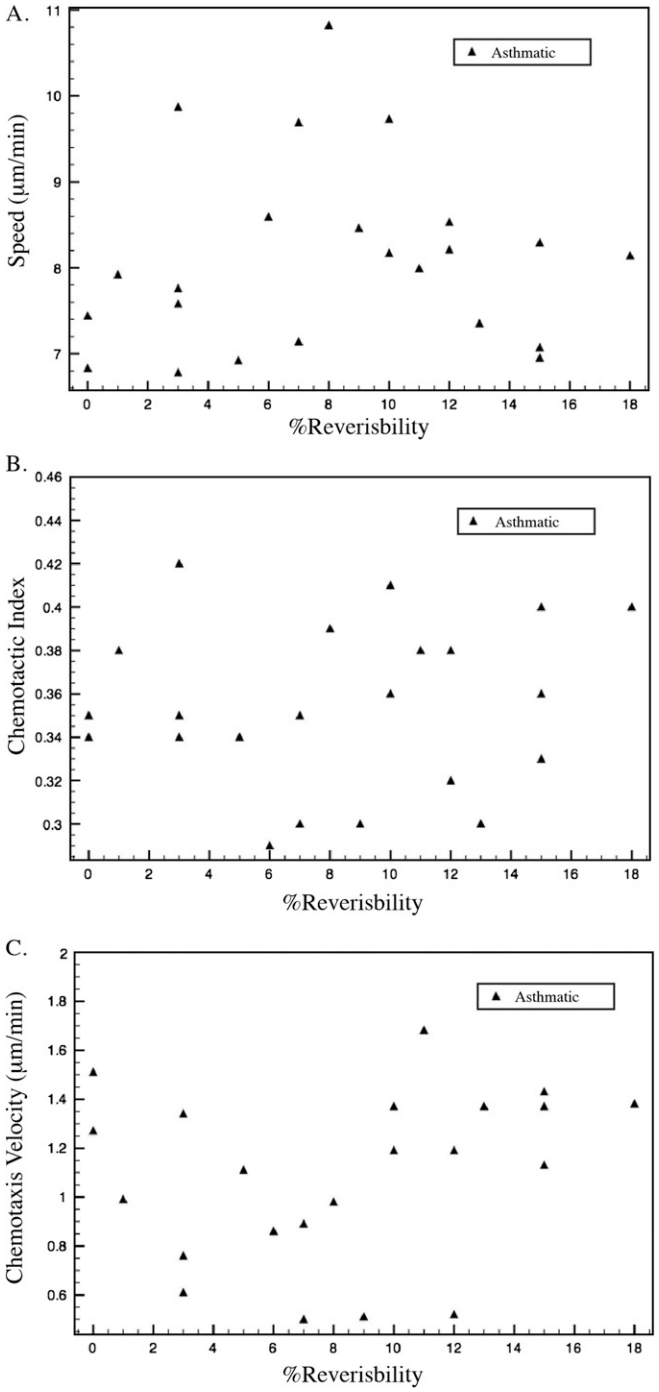

Fig. S6. The %Reversibility compared with neutrophil chemotaxis speed (*A*), chemotactic index (*B*), and (*C*) chemotaxis velocity. Only asthmatic patients are reported, because insufficient data are available for nonasthmatic patients.

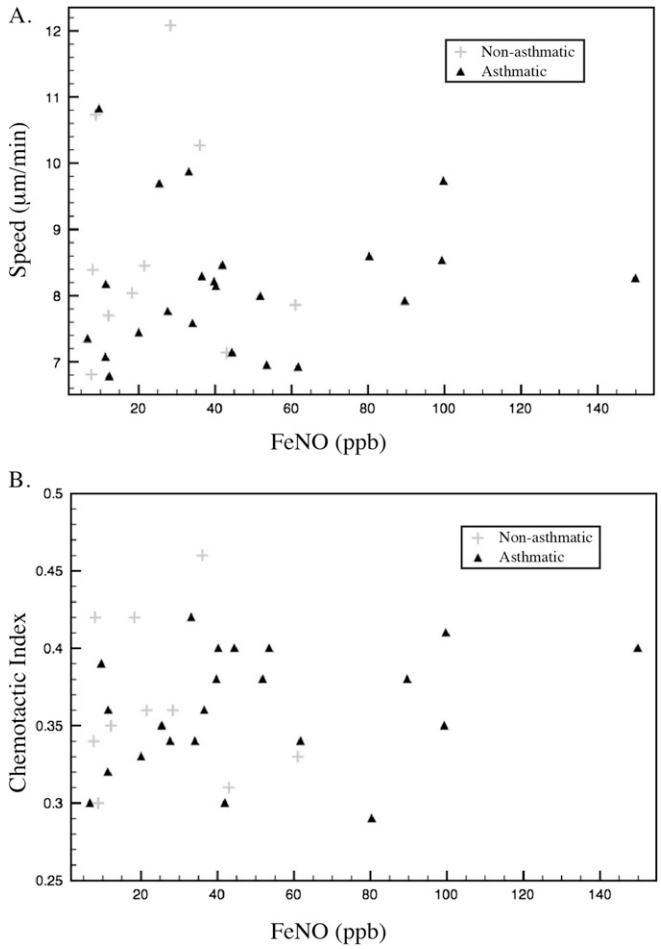

Fig. S7. FeNO compared with neutrophil chemotaxis speed (*A*) and chemotactic index (*B*). No apparent correlations between the neutrophil chemotaxis outputs and FeNO values.

Table S1. Comparative diagnostic performance of other methods compared with microfluidic test

Diagnostic test	Cutoff	Sensitivity	Specificity	Ref.
FeNO, ppb	46	32	93	1
	20	77	64	2
	20	64	59	3
	47	42	96	–
	13	85	80	4
	19	85	52	5
	40	79	90	6
	20	67	52	7
%EOS, BAL	3	41	75	2
	1	72	80	8
	5	85	92	9
PC20	8 mg/mL	91	90	8
	–	78	94	3
	16 mg/mL	41	85	2
FEV1	80	22	100	2
FEV1/FVC	76.6%	61	60	8
Chemotaxis test	1.545 μm/min	96	73	–

BAL, bronchoalveolar lavage; %EOS, eosinophil count; PC20, provocative concentration that reduces FEV by 20%.

1. Schneider A, et al. (2009) Diagnosing asthma in general practice with portable exhaled nitric oxide measurement—results of a prospective diagnostic study: FENO < or = 16 ppb better than FENO < or =12 ppb to rule out mild and moderate to severe asthma. *Respir Res* 10:15, and erratum 10:64.
2. Fortuna AM, Feixas T, González M, Casan P (2007) Diagnostic utility of inflammatory biomarkers in asthma: Exhaled nitric oxide and induced sputum eosinophil count. *Respir Med* 101(11):2416–2421.
3. Miedinger DD, et al. (2007) Diagnostic tests for asthma in firefighters. *Chest* 131(6):1760–1767.
4. Dupont LJ, Demedts MG, Verleden GM (2003) Prospective evaluation of the validity of exhaled nitric oxide for the diagnosis of asthma. *Chest* 123(3):751–756.
5. Kostikas K, et al. (2008) Portable exhaled nitric oxide as a screening tool for asthma in young adults during pollen season. *Chest* 133(4):906–913.
6. Fukuhara A, et al. (2011) Validation study of asthma screening criteria based on subjective symptoms and fractional exhaled nitric oxide. *Ann Allergy Asthma Immunol* 107(6):480–486.
7. Menzies D, Jackson C, Mistry C, Houston R, Lipworth BJ (2008) Symptoms, spirometry, exhaled nitric oxide, and asthma exacerbations in clinical practice. *Ann Allergy Asthma Immunol* 101(3):248–255.
8. Hunter CJ, Brightling CE, Woltmann G, Wardlaw AJ, Pavord ID (2002) A comparison of the validity of different diagnostic tests in adults with asthma. *Chest* 121(4):1051–1057.
9. Park JWJ, Whang YWY, Kim CWC, Park YBY, Hong CSC (1998) Eosinophil count and eosinophil cationic protein concentration of induced sputum in the diagnosis and assessment of airway inflammation in bronchial asthma. *Allergy Asthma Proc* 19(2):61–67.

Table S2. Medications taken by asthmatic and non-asthmatic patients

Patient (generic name)	Asthma?	Current symptoms?	Chemotaxis Velocity (μm/min)	Medications
P01	N	N	2.46	
P02	Y	N	0.61	
P03	Y	N	1.13	Zoloft, Symbicort, Trazadone
P04	Y	N	1.37	Zyrtec, Lisinopril
P05	Y	N	1.38	Albuterol Sulfate
P06	N	N	0.46	
P07	Y	N	1.19	Tylenol Severe Allergies, Primatene Mist
P08	Y	N	0.98	Flovent, Albuterol, Zyrtec, Multivitamins, Verapamil, Trisprintec, Sertaline, Nasonex
P09	Y	N	0.51	Multivitamin, Mirena, Prilosec
P10	Y	N	1.00	Yasmin
P11	Y	N	1.34	Clonazepam, Chlorphenamine
P12	N	N	2.53	
P13	Y	N	1.68	
P14	Y	N	1.15	
P15	N	N	3.14	
P16	Y	N	0.89	
P17	Y	Y	1.43	Symbicort, Trazadone, Claritin, Ibuprofin, Zoloft
P18	N	N	1.61	
P19	Y	N	1.37	
P20	N	N	2.48	Prilosec, Celexa
P21	Y	N	0.52	Albuterol Sulfate, Advair Diskus 100/50, Pulmicort
P22	Y		1.27	Desogen, Patanol
P23	Y	N	1.19	
P24	Y	N	1.37	Albuterol, Nasonex, Ibuprofen
P25	N	N	1.20	Cetrizine
P26	Y	N	1.51	Ortho Cyclen-21, Ibuprofen
P27	Y	N	0.76	Albuterol Sulfate, Chlorphenamine, Celexa
P28	N	N	1.28	Metformin, Yaz, Iron Supplement
P29	Y	N	0.86	Albuterol
P30	N	N	1.58	Aleve, Aspirin, Multivitamin
P31	Y	N	0.50	Benadryl, Multivitamins
P32	N	N	1.65	Azurette, Nirtrofurantoin Macrocrystalline
P33	N	N	2.40	
P34	Y	N	1.11	Oral Contraceptives, Tylenol, Multivitamin

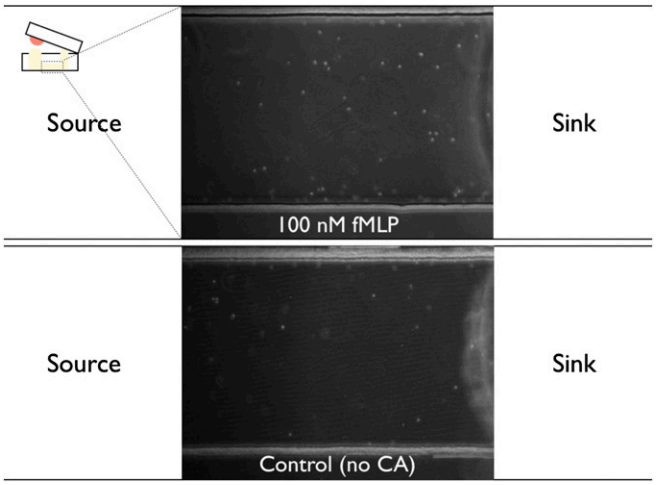

Movie S1. An example of human neutrophils from a clinical patient sample migrating in a gradient of chemoattractant, compared with the control (no chemoattractant). Human neutrophils migrating toward 100 nM fMLP on P-selectin–coated polystyrene or inactivated in control case with hydrogel and media (no chemoattractant). Note that some erythrocyte movement is observable over the course of the time lapse, likely due to a temperature gradient in the microscope incubator causing slight fluid convection. The time lapse is 90 min long. The source of chemoattractant is located on the left side of the movie. Phase contrast images acquired using SlideBook software with an Olympus IX-81 microscope using a 10× objective (N.A. = 0.30) at 37 °C.

Movie S1

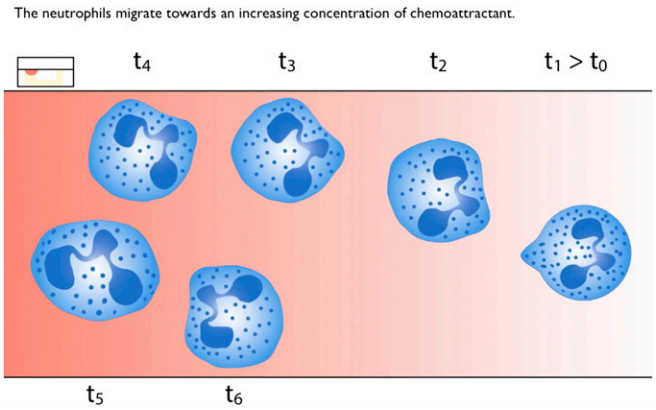

Movie S2. Interactive video (click through) shows, step by step, how automated tracking software identifies neutrophils and generates chemotaxis outputs.

Movie S2

Dataset S1. Workflow of performing the microfluidic assay

Dataset S1